Monthly Notices of the ROYAL ASTRONOMICAL SOCIETY LETTERS

Mon. Not. R. Astron. Soc. **425,** L66–L70 (2012) doi:10.1111/j.1745-3933.2012.01303.x

Evidence of strong quasar feedback in the early Universe

R. Maiolino,[1⋆] S. Gallerani,[2] R. Neri,[3] C. Cicone,[1] A. Ferrara,[2] R. Genzel,[4] D. Lutz,[4] E. Sturm,[4] L. J. Tacconi,[4] F. Walter,[5] C. Feruglio,[3] F. Fiore[6] and E. Piconcelli[7]

[1]*Cavendish Laboratory, University of Cambridge, 19 J. J. Thomson Avenue, Cambridge CB3 0HE*
[2]*Scuola Normale Superiore, Piazza dei Cavalieri 7, 56126 Pisa, Italy*
[3]*Institute de Radioastronomie Millimetrique (IRAM), 300 Rue de la Piscine, 38406 St. Martin d'Heres, Grenoble, France*
[4]*Max-Planck-Institut für Extraterrestrische Physik (MPE), Giessenbachstr. 1, 85748 Garching, Germany*
[5]*Max-Planck-Institut für Astronomie, Königstuhl 17, 69177 Heidelberg, Germany*
[6]*Osservatorio Astronomico di Roma, INAF, via di Frascati 33, 00040 Monteporzio Catone, Italy*
[7]*ESA-ESAC, Camino bajo del Castillo, Villanueva de la Canada, E-28692 Madrid, Spain*

Accepted 2012 June 12. Received 2012 June 12; in original form 2012 March 29

ABSTRACT

Most theoretical models invoke quasar-driven outflows to quench star formation in massive galaxies, and this feedback mechanism is required to account for the population of old and passive galaxies observed in the local Universe. The discovery of massive, old and passive galaxies at $z \sim 2$ implies that such quasar feedback on to the host galaxy must have been at work very early on, close to the reionization epoch. We have observed the [C II] 158 μm transition in SDSS J114816.64+525150.3, which, at $z = 6.4189$, is one of the most distant quasars known. We detect broad wings of the line tracing a quasar-driven massive outflow. This is the most distant massive outflow ever detected and is likely tracing the long-sought quasar feedback, already at work in the early Universe. The outflow is marginally resolved on scales of ∼16 kpc, implying that the outflow can really affect the whole galaxy, as required by quasar feedback models. The inferred outflow rate, $\dot{M} > 3500\,\mathrm{M}_\odot\,\mathrm{yr}^{-1}$, is the highest ever found. At this rate, the outflow can clean the gas in the host galaxy, and therefore quench star formation, in a few million years.

Key words: galaxies: evolution – galaxies: high-redshift – quasars: general.

1 INTRODUCTION

The old stellar population and low gas content characterizing local massive galaxies, as well as their steeply declining number at high masses, have been difficult to explain in most theoretical scenarios of galaxy formation. Indeed, in the absence of 'negative feedback' on star formation (i.e. a mechanism to decrease star formation), theoretical models expect a much larger number of massive galaxies than observed and characterized by young stellar populations (Bower et al. 2006; Menci et al. 2006). To reconcile theory with observations, most models invoke massive outflows driven by the radiation pressure generated by quasars, which are expected to clear their host galaxies of the bulk of their gas, therefore quenching star formation (Silk & Rees 1998; Granato et al. 2004; Di Matteo, Springel & Hernquist 2005; Springel, Di Matteo & Hernquist 2005; Croton et al. 2006; Hopkins et al. 2008; Narayanan et al. 2008; Fabian et al. 2009; Hopkins & Elvis 2010; King 2010; King, Zubovas & Power 2011; Zubovas & King 2012). Evidence for such negative feedback has been found only recently in quasar hosts through the discovery of massive outflows, in particular through the detection of P Cygni profiles of far-infrared (far-IR) OH transitions (Fischer et al. 2010; Sturm et al. 2011), the detection high-velocity wings of molecular emission lines (CO, HCN; Feruglio et al. 2010; Alatalo et al. 2011; Aalto et al. 2012) and the detection of high-velocity neutral gas in absorption and of high-velocity ionized gas (Nesvadba et al. 2010; Greene et al. 2011; Rupke & Veilleux 2011). Evidence for quasar-driven massive outflows has also been found through the bright [C II] 158 μm fine structure line; indeed, *Herschel* spectra of nearby quasars have revealed prominent [C II] broad wings, associated with the molecular outflow traced by the OH absorption lines (Fischer et al. 2010; Sturm et al., in preparation). Quasar-driven outflows have been detected also at high redshift (although exploiting different tracers; Alexander et al. 2010; Nesvadba et al. 2011; Harrison et al. 2012). Moreover, evidence has been found that these outflows are indeed quenching star formation in their host galaxies (Steinhardt & Silverman 2011; Cano-Díaz et al. 2012; Farrah et al. 2012; Page et al. 2012), as expected by models.

However, the discovery of old (age > 2 Gyr), passive and massive galaxies at $z \sim 2$ (Cimatti et al. 2004; Glazebrook et al. 2004; McCarthy et al. 2004; Saracco et al. 2005), when the Universe had

⋆E-mail: r.maiolino@mrao.cam.ac.uk

an age of only ∼3 Gyr, requires that the quasar feedback quenching mechanism must have been at work already at $z > 6$ (age of the Universe less than 1 Gyr), i.e. close to the reionization epoch. Quasar-driven winds have been observed up to $z \sim 6$ (Maiolino et al. 2001, 2004); however, these are associated with ionized gas in the vicinity of the black hole, accounting only for a tiny fraction of the total gas in the host galaxy. So far, no observational evidence was found for the massive, quasar-driven outflows at $z > 6$ required by feedback models to explain the population of old massive galaxies at $z \sim 2$.

Here we focus on one of the most distant quasars known, SDSS J114816.64+525150.3 (hereafter J1148+5251), at $z = 6.4189$ (Fan et al. 2003). CO observations have revealed a large reservoir of molecular gas, $M_{H_2} \sim 2 \times 10^{10}\,M_\odot$, in the quasar host galaxy (Bertoldi et al. 2003b; Walter et al. 2003). The strong far-IR thermal emission inferred from (sub)millimetre observations reveals vigorous star formation in the host galaxy, with star formation rate (SFR) $\sim 3000\,M_\odot\,yr^{-1}$ (Bertoldi et al. 2003a; Beelen et al. 2006). J1148+5251 is also the first high-redshift galaxy in which the [C II] 158 μm line was discovered (Maiolino et al. 2005). High-resolution mapping of the same line with the Institute de Radioastronomie Millimetrique (IRAM) Plateau de Bure Interferometer (PdBI) revealed that most of the emission is confined within ∼1.5 kpc, indicating that most of the star formation is occurring within a very compact region (Walter et al. 2009).

Previous [C II] observations of J1148+5251 did not have a bandwidth large enough to allow the investigation of broad wings tracing outflows, as in local quasars. In this Letter, we present new IRAM PdBI observations of J1148+5251 that, thanks to the wide bandwidth offered by the new correlator, have allowed us to discover broad [C II] wings tracing a very massive and energetic outflow in the host galaxy of this early quasar. We show that the properties of this outflow are consistent with the expectations of quasar feedback models.

We assume the concordance Λ-cosmology with $H_0 = 70.3\,km\,s^{-1}\,Mpc^{-1}$, $\Omega_\Lambda = 0.73$ and $\Omega_m = 0.27$ (Komatsu et al. 2011).

2 OBSERVATIONS AND DATA REDUCTION

Observations with the IRAM PdBI were obtained mostly in 2011 April in D configuration (mostly with precipitable water vapor (PWV) in the range 1.5–3.5 mm), while a few hours were also obtained in 2011 January in C+D configuration (PWV < 1.5 mm). The resulting synthesized beam is $2.2 \times 1.8\,arcsec^2$. The receivers were tuned to 256.172 GHz, which is the rest-frame frequency of [C II] at the redshift of the quasar, $z = 6.4189$ (Maiolino et al. 2005). The following flux calibrators were used: 3C 454.3, MWC 349, 0923+392, 1150+497, 3C 273, 3C 345, 1144+542, J1208+546, J1041+525 and 1055+018. Uncertainties on the absolute flux calibration are 20 per cent. The total on-source integration time was 17.5 h, resulting in a sensitivity of $0.08\,Jy\,km\,s^{-1}\,beam^{-1}$ in a channel with width $100\,km\,s^{-1}$.

The data were reduced by using the CLIC and MAPPING packages, within the IRAM GILDAS software. Cleaning of the resulting maps was run by selecting the clean components on an area of ∼3 arcsec around the peak of the emission. For each map, the resulting residuals are below the 1σ error, ensuring that sidelobes are properly cleaned away. Anyhow, as discussed in the following, the size determination has been investigated directly on the *uv* data, therefore independently of the cleaning.

3 RESULTS

3.1 Detection of broad wings

The continuum was subtracted from the *uv* data by estimating its level from the channels at $v < -1300\,km\,s^{-1}$ and at $v > +1300\,km\,s^{-1}$. The inferred continuum flux is 3.7 mJy, which is fully consistent with the value expected (4 mJy) from the bolometric observations (Bertoldi et al. 2003a), once the frequency range of the latter and the steep shape of the thermal spectrum are taken into account.

Fig. 1(a) shows the continuum-subtracted spectrum, extracted from an aperture of 4 arcsec (corresponding to a physical size of 11 kpc). Fig. 1(b) shows the spectrum extracted from a larger aperture of 6 arcsec that, although noisier than the former spectrum, recovers residual flux associated with the beam wings and with any extended component.

The spectrum shows a clear narrow [C II] 158 μm emission line, which was already detected by previous observations (Maiolino

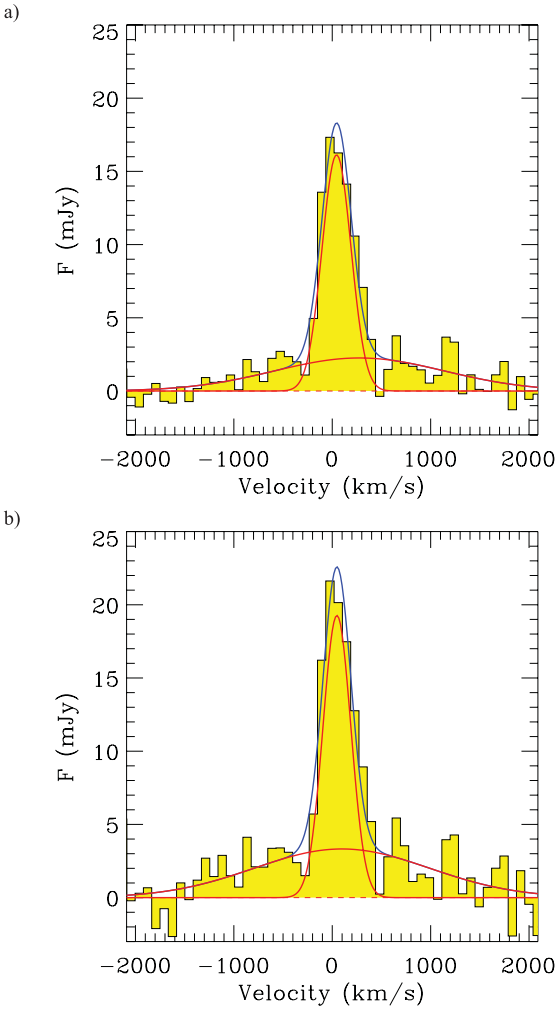

Figure 1. IRAM PdBI continuum-subtracted spectrum of the [C II] 158 μm line, redshifted to 256.172 GHz, in the host galaxy of the quasar J1148+5152 extracted from an aperture with a diameter of 4 arcsec (top) and 6 arcsec (bottom). The spectrum has been resampled to a bin size of $85\,km\,s^{-1}$. The red lines show a double Gaussian fit (FWHM = 345 and $2030\,km\,s^{-1}$) to the line profile, while the blue line shows the sum of the two Gaussian components.

et al. 2005; Walter et al. 2009). However, thanks to the much wider bandwidth relative to previous data, our new spectrum reveals broad [C II] wings extending to about $\pm 1300\,\mathrm{km\,s^{-1}}$. These are indicative of a powerful outflow, in analogy with the broad wings that have been observed in the molecular and fine structure lines of local quasar host galaxies. The spectrum is fitted[1] with a narrow [full width at half-maximum (FWHM) $= 345\,\mathrm{km\,s^{-1}}$] and a broad (FWHM $= 2030\,\mathrm{km\,s^{-1}}$) Gaussian, as shown in Fig. 1, resulting into $\chi^2_{\rm red} = 1.11$. By removing the broad component, the χ^2 increases from 195 to 229 (with 175 degrees of freedom), implying that the broad component is required at a confidence level higher than 99.9 per cent.

Theoretical models predict that starburst-driven winds cannot reach velocities higher than $600\,\mathrm{km\,s^{-1}}$ (Martin 2005; Thacker, Scannapieco & Couchman 2006); therefore, the high velocities observed in the [C II] wings of J1148+5251 strongly favour radiation pressure from the quasar nucleus as the main driving mechanism of the outflow. Quasar radiation pressure is favoured, relative to supernova-driven winds, also based on energetics arguments, as discussed later on.

3.2 Outflowing gas mass

The luminosity of the broad [C II] component allows us to infer a lower limit of the outflowing atomic gas mass, using

$$\frac{M_{\rm outfl}({\rm atomic})}{\rm M_\odot} = 0.77 \left(\frac{0.7 L_{\rm [C\,II]}}{\rm L_\odot}\right)\left(\frac{1.4\times10^{-4}}{X_{\rm C^+}}\right) \times \frac{1+2{\rm e}^{-91K/T}+n_{\rm crit}/n}{2{\rm e}^{-91K/T}} \quad (1)$$

(Hailey-Dunsheath et al. 2010), where $X_{\rm C^+}$ is the $\rm C^+$ abundance per hydrogen atom, T is the gas temperature, n is the gas density and $n_{\rm crit}$ is the critical density of the [C II] 158 μm transition ($\sim 3\times10^3\,\mathrm{cm^{-3}}$). By assuming a density much higher than the critical density, equation (1) gives a lower limit on the mass of atomic gas. The quasar-driven outflows observed locally are characterized by a wide range of densities, including both dense clumps and diffuse, low-density gas (Fischer et al. 2010; Aalto et al. 2012; Cicone et al. 2012); therefore, our assumption on the gas density gives a conservative lower limit on the outflowing gas mass. We assume a temperature of 200 K; however, the dependence on the temperature is weak (going from 100 to 1000 K, the implied gas mass is within 20 per cent of the value obtained at 200 K). Furthermore, we assume a $\rm C^+$ abundance typical of photodissociation regions (PDRs, i.e. $X_{\rm C^+} = 1.4\times10^{-4}$ (Savage & Sembach 1996), which is also conservative, since the gas in the outflow is certainly, on average, at a higher state of ionization. The luminosity of the [C II] broad component is inferred from the flux of this component in the spectrum extracted from an aperture of 6 arcsec [$F_{\rm [C\,II]}({\rm broad}) = 6.8\,\mathrm{Jy\,km\,s^{-1}}$], yielding $L_{\rm [C\,II]}({\rm broad}) = 7.3\pm0.9\times10^9\,\rm L_\odot$. We obtain a lower limit on the outflowing atomic gas mass of

$$M_{\rm outfl}({\rm atomic}) > 7\times10^9\,\rm M_\odot\,. \quad (2)$$

We emphasize that this is a conservative lower limit on the total mass of outflowing gas, not only because of the assumptions on the physical properties of the outflowing atomic gas, but also because a significant fraction of the outflowing gas is likely in the molecular form.

[1] Note that, although Fig. 1 shows the spectrum resampled in channels of $85\,\mathrm{km\,s^{-1}}$ for the sake of clarity, the fit was performed on the unbinned spectrum to avoid any fitting artefact associated with the binning.

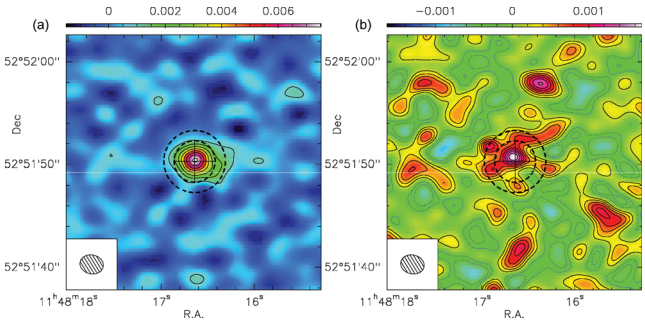

Figure 2. Map of the continuum-subtracted [C II] line narrow component (a), $-300 < v < +400\,\mathrm{km\,s^{-1}}$, and of the [C II] line wings (b), $-1300 < v < -300\,\mathrm{km\,s^{-1}}$ and $+400 < v < +1300\,\mathrm{km\,s^{-1}}$. See text for details on the continuum subtraction of the narrow component. The dashed circles indicate the extraction apertures of the two spectra shown in Fig. 1. Levels are in steps of $0.64\,\mathrm{Jy\,km\,s^{-1}\,beam^{-1}}$ (i.e. 3σ) in the narrow component map (a) and in steps of $0.36\,\mathrm{Jy\,km\,s^{-1}\,beam^{-1}}$ (i.e. 1σ) in the broad wings map (b). The beam of the observation is shown in the bottom-left corner. At the redshift of the source, 1 arcsec corresponds to 5.5 kpc. The colour bars are in units of $\mathrm{Jy\,beam^{-1}}$, giving the average flux density in each velocity integration interval; to obtain fluxes in units of $\mathrm{Jy\,km\,s^{-1}\,beam^{-1}}$, one has to multiply by the width of the integration interval of each map.

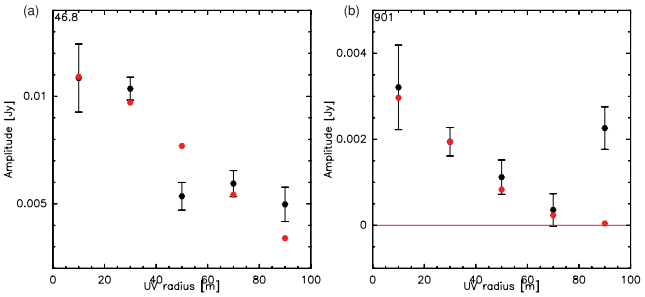

Figure 3. Amplitude of the visibilities as a function of the baseline distance (black symbols) for the narrow component of the [C II] line (a) and for its broad wings (b). In both cases, the distribution of visibilities is inconsistent with an unresolved source (which would give a flat distribution). The red symbols show the result of the best fit by using a circular Gaussian model. Note that the units (Jy) refer to the average flux in the selected channels associated with the line; to obtain the units in terms of line flux, one has to multiply by 700 and by $1800\,\mathrm{km\,s^{-1}}$, respectively.

3.3 Extension

Fig. 2(a) shows the map of the [C II] narrow component integrated within[2] $-300 < v < +400\,\mathrm{km\,s^{-1}}$. Note that in this case we have subtracted a pseudo-continuum defined by the flux observed at $400 < |v| < 800\,\mathrm{km\,s^{-1}}$ (resulting in a level of 5.6 mJy), to minimize the contribution of the broad component. Fig. 2(b) shows the map of the [C II] broad wings, where we have combined the blue ($-1300 < v < -300\,\mathrm{km\,s^{-1}}$) and red ($+400 < v < +1300\,\mathrm{km\,s^{-1}}$) wings to improve the signal-to-noise ratio.

The narrow component (Fig. 2a), tracing gas and star formation in the host galaxy, is resolved at high significance. To illustrate this extension more quantitatively, Fig. 3(a) shows the amplitude of the visibilities as a function of the baseline distance (black symbols) for the narrow component of the [C II] line. Error bars show the statistical photon noise on the average amplitude in each bin.

[2] The line core integration limits are asymmetric because the narrow component is slightly skewed towards positive velocities.

In this diagram, an unresolved source has a flat distribution. Such a flat distribution can be ruled out by the *uv* data. A fit of the *uv* data with a simple circular Gaussian gives a size $FWHM = 1.5$ arcsec, corresponding to 8 kpc. However, as illustrated by the red symbols, showing the result of the fit, a single circular Gaussian does not provide a good description of the data, indicating that the morphology of the [C II] core emission is more complex. We know that the [C II] core has a very compact component (size 0.3 arcsec; Walter et al. 2009) which is unresolved at our resolution. This compact component is responsible for the flat visibilities at baselines longer than 40 m. The rising visibilities at baselines shorter than 40 m indicate the presence of a resolved component, with size larger than 2 arcsec, whose flux is about 40 per cent of the total narrow line flux. It is likely that this extended component of the narrow [C II] emission was resolved out in previous high angular resolution observations.

The spatial extension of the line wings is more difficult to quantify due the lower signal-to-noise ratio. The map of the wings (Fig. 2b) is characterized by a compact core, detected at 8σ, and diffuse emission surrounding the source on scales of a few arcsec, but at low significance. The amplitude versus *uv* radius diagram, shown in Fig. 3(b), suggests that the outflow is indeed marginally resolved, as indicated by the decreasing visibilities out to 70 m. The visibilities at distances <70 m are inconsistent with a flat distribution at confidence level higher than 99 per cent. A fit of the *uv* visibilities with a simple circular Gaussian (shown with the red symbols) gives a size of 2.9 arcsec (16 kpc). If confirmed (with higher resolution and deeper observations), this would be the largest outflow ever detected and it would support models ascribing the capability of cleaning entire galaxies, out to large radii, to quasar-driven outflows. However, the intensity of the last visibility at 90 m suggests that the structure of the outflow is more complex and cannot be modelled with a simple Gaussian. We have attempted to fit a ring-like morphology to the *uv* data, but the fit does not improve and the inner radius is set to a very small value (<0.1 arcsec).

Finally, we note that the fit also requires an offset of the core of the wings of 0.3 arcsec (±0.1 arcsec) relative to the line core; this is also observed in the map (Fig. 2b). The offset is small and marginally significant. However, even if real, an offset of the centroid of the outflowing gas is not surprising, since outflows observed in local and high-z galaxies are not aligned with the galaxy centres (Weiß et al. 2001; Walter, Dahlem & Lisenfeld 2004; Wilson et al. 2008; Alatalo et al. 2011).

3.4 Outflow rate, energetics and depletion time

Given the limited information available, we cannot elaborate on sophisticated models. We have assumed a simple scenario where the outflow occurs in a spherical volume (or conical or multiconical volume), with radius $R_{\rm outflow}$, uniformly filled with outflowing clouds. Note that the outflowing clouds can have any density distribution, since we are assuming the conservative case of $n \gg n_{\rm crit}$, which gives a lower limit on the outflowing mass according to equation (1). The presence of clouds with density below the critical density would result into an even higher outflow mass and outflow rate.

For the geometry discussed above, the volume-averaged density of atomic gas in the outflow is $\langle\rho_{\rm outfl}\rangle_{\rm V} = 3M_{\rm outfl}/(\Omega R^3_{\rm outfl})$, where Ω is the total solid angle subtended by the (multi)conical outflow ($\Omega = 4\pi$ for a spherical outflow). Note that $\langle\rho_{\rm outfl}\rangle_{\rm V}$ should not be confused with the gas density of the individual clouds. In the case of a shell (or fragmented shell) geometry, the volume-averaged density is $\langle\rho_{\rm outfl}\rangle_{\rm V} = 3M_{\rm outfl}/[\Omega(R^3_{\rm outfl} - R^3_{\rm in})] \approx M_{\rm outfl}/(\Omega R^2_{\rm outfl}{\rm d}R)$, where $R_{\rm in}$ is the inner radius of the shell and where the last approximation holds in the case that the shell thickness (${\rm d}R = R_{\rm outfl} - R_{\rm in}$) is much smaller than its radius. In these equations, Ω is the total solid angle subtended by the (fragmented) shell.

In the case of a spherical, or multiconical, geometry, the outflow rate is then given by

$$\dot{M}_{\rm outfl} \approx v\Omega R^2_{\rm outfl}\langle\rho_{\rm outfl}\rangle_{\rm V} = 3v\frac{M_{\rm outfl}}{R_{\rm outfl}}, \quad (3)$$

where v is the outflow velocity. In the case of a (fragmented) shell-like geometry,

$$\dot{M}_{\rm outfl} \approx 3v\frac{R^2_{\rm outfl}M_{\rm outfl}}{R^3_{\rm outfl} - R^3_{\rm inner}} \approx v\frac{M_{\rm outfl}}{{\rm d}R}. \quad (4)$$

Clearly, the shell-like geometry gives an even higher outflow rate relative to the spherical/multiconical geometry. In the following, we conservatively assume the latter geometry. Note also that the outflow rate is independent of Ω, both in the (multi)conical and in the (fragmented) shell geometries.

Since we have a lower limit on $M_{\rm outfl}$, we can derive a conservative lower limit on the outflow rate. In particular, by taking $R_{\rm outfl} = 8$ kpc and $v = 1300\,{\rm km\,s^{-1}}$ (conservatively assuming that the maximum velocity observed in the wings is the deprojected velocity of the outflow, which is a lower limit in the case of a conical outflow not intercepting the plane of the sky), we obtain

$$\dot{M}_{\rm outfl} > 3500\,{\rm M_\odot\,yr^{-1}}. \quad (5)$$

We note that if the outflow size has been overestimated, due to the low signal-to-noise ratio in the wings, as discussed above, and the bulk of the flux is actually unresolved, then the lower limit on the outflow rate in equation (5) is even more conservative, since the outflow rate scales as $1/R_{\rm outfl}$. As discussed above, a (fragmented) shell-like geometry would give an even higher outflow rate. Concerning the velocity field, the angular resolution of our data does not allow us to map the kinematics of the outflow. However, we note that, in the nearby quasar Mrk 231, transitions tracing the outflow on different scales have the same profile and the same maximum velocity (Aalto et al. 2012; Cicone et al. 2012), supporting the scenario where quasar-driven outflows have velocity roughly constant throughout the wind. The same kinematics is likely to apply to J1148+5251 as well. However, new higher angular resolution observations will allow us to better constrain the kinematics.

The inferred lower limit on the outflow rate is similar to the SFR in the host galaxy ($\sim$3000 ${\rm M_\odot\,yr^{-1}}$).

The kinetic power associated with the outflow is given by

$$P_{\rm K} \approx 0.5v^2\dot{M}_{\rm outfl} > 1.9\times10^{45}{\rm erg\,s^{-1}}, \quad (6)$$

which is about 0.6 per cent of the bolometric luminosity of the quasar nucleus. On the one hand, this is well below the maximum efficiency expected for quasars to drive outflows ($P_{\rm K}/L_{\rm bol} \sim 5$ per cent; Lapi, Cavaliere & Menci 2005), meaning that the quasar radiation pressure is probably fully capable of driving the outflow observed in J1148+5251. On the other hand, the lower limit on the outflow kinetic power is barely consistent with the kinetic power that can be achieved by a starburst-driven wind [$P_{\rm K}({\rm SB}) = 7\times10^{41}\,({\rm SFR/M_\odot\,yr^{-1}})\,{\rm erg\,s^{-1}} \approx 2\times10^{45}\,{\rm erg\,s^{-1}}$ for J1148+5152; Veilleux, Cecil & Bland-Hawthorn 2005]; therefore, we cannot exclude a starburst contribution to the wind based solely on energetic arguments and by using simple scaling equations. However, as discussed above, the very high outflow velocities are difficult to explain by starburst-driven wind models, hence strongly favouring quasar radiation pressure as the main driving mechanism.

We also mention that a parallel paper (Valiante, Schneider & Maiolino 2012), by exploiting existing detailed cosmological models specifically suited for J1148+5251 constrained by all observable quantities, does predict a quasar-driven wind fully consistent with the outflow rate measured by us, while the outflow contribution by the starburst is orders of magnitude lower.

The molecular gas content in the host galaxy of J1148+5251, as inferred by CO observations, is $2 \times 10^{10}\,M_\odot$ (Bertoldi et al. 2003b; Walter et al. 2003). At the observed (minimum) outflow rate, the quasar host galaxy will be cleaned of its gas content, hence quenching star formation, within less than 6×10^6 yr.

4 CONCLUSIONS

By using the IRAM PdBI, we have discovered an exceptional outflow in the host galaxy of the quasar J1148+5251 at $z = 6.4$, through the detection of prominent broad wings of the [C II] 158 μm line, with velocities up to about $\pm 1300\,km\,s^{-1}$. This is the most distant massive outflow ever detected and it is likely tracing the long-sought quasar-feedback already in place in the early Universe, close to the reionization epoch. Both the high outflow velocity and the kinetic power ($P_K > 1.9 \times 10^{45}$ erg s^{-1}) favour quasar radiation pressure as the main driving mechanism. A more detailed cosmological model of J1148+5251 (Valiante et al. 2012) confirms that in this object a quasar-driven outflow is expected with an outflow rate consistent with what observed by us, while the contribution from the starburst wind is orders of magnitude lower.

We marginally resolve the outflow, with a size of about 16 kpc, which would make it the largest outflow ever detected. This finding supports models ascribing the capability of cleaning entire galaxies, out to large radii, to quasar-driven outflows. However, higher angular resolution and deeper observations are required to confirm the outflow extension.

We infer a conservative lower limit on the total outflow rate of $\dot{M}_{outfl} > 3500\,M_\odot\,yr^{-1}$, which would be the highest outflow rate ever detected. This lower limit on the outflow rate is higher than the SFR in the quasar host (SFR $\approx 3000\,M_\odot\,yr^{-1}$). At the observed outflow rate, the gas content in the host galaxy will be cleaned, and therefore star formation will be quenched, in less than 6×10^6 yr. Such a fast and efficient quenching mechanism, already at work at $z > 6$, is what is required by models to explain the properties of massive, old and passive galaxies observed in the local Universe and at $z \sim 2$.

ACKNOWLEDGMENTS

This work is based on observations carried out with the IRAM Plateau de Bure Interferometer. IRAM is supported by INSU/CNRS (France), MPG (Germany) and IGN (Spain). We are grateful to A. Marconi for useful comments. SG thanks INAF for support through an International Post-Doctoral Fellowship.

REFERENCES

Aalto S., Garcia-Burillo S., Muller S., Winters J. M., van der Werf P., Henkel C., Costagliola F., Neri R., 2012, A&A, 537, A44
Alatalo K. et al., 2011, ApJ, 735, 88
Alexander D. M., Swinbank A. M., Smail I., McDermid R., Nesvadba N. P. H., 2010, MNRAS, 402, 2211
Beelen A., Cox P., Benford D. J., Dowell C. D., Kovács A., Bertoldi F., Omont A., Carilli C. L., 2006, ApJ, 642, 694
Bertoldi F., Carilli C. L., Cox P., Fan X., Strauss M. A., Beelen A., Omont A., Zylka R., 2003a, A&A, 406, L55
Bertoldi F. et al., 2003b, A&A, 409, L47
Bower R. G., Benson A. J., Malbon R., Helly J. C., Frenk C. S., Baugh C. M., Cole S., Lacey C. G., 2006, MNRAS, 370, 645
Cano-Díaz M., Maiolino R., Marconi A., Netzer H., Shemmer O., Cresci G., 2012, A&A, 537, L8
Cicone C., Feruglio C., Maiolino R., Fiore F., Piconcelli E., Menci N., Aussel H., Sturm E., 2012, A&A, in press (arXiv:1204.5881)
Cimatti A. et al., 2004, Nat, 430, 184
Croton D. J. et al., 2006, MNRAS, 365, 11
Di Matteo T., Springel V., Hernquist L., 2005, Nat, 433, 604
Fabian A. C., Vasudevan R. V., Mushotzky R. F., Winter L. M., Reynolds C. S., 2009, MNRAS, 394, L89
Fan X. et al., 2003, AJ, 125, 1649
Farrah D. et al., 2012, ApJ, 745, 178
Feruglio C., Maiolino R., Piconcelli E., Menci N., Aussel H., Lamastra A., Fiore F., 2010, A&A, 518, L155
Fischer J. et al., 2010, A&A, 518, L41
Glazebrook K. et al., 2004, Nat, 430, 181
Granato G. L., De Zotti G., Silva L., Bressan A., Danese L., 2004, ApJ, 600, 580
Greene J. E., Zakamska N. L., Ho L. C., Barth A. J., 2011, ApJ, 732, 9
Hailey-Dunsheath S., Nikola T., Stacey G. J., Oberst T. E., Parshley S. C., Benford D. J., Staguhn J. G., Tucker C. E., 2010, ApJ, 714, L162
Harrison C. M. et al., 2012, MNRAS, in press (arXiv:1205.1801)
Hopkins P. F., Elvis M., 2010, MNRAS, 401, 7
Hopkins P. F., Cox T. J., Kereš D., Hernquist L., 2008, ApJS, 175, 390
King A. R., 2010, MNRAS, 402, 1516
King A. R., Zubovas K., Power C., 2011, MNRAS, 415, L6
Komatsu E. et al., 2011, ApJS, 192, 18
Lapi A., Cavaliere A., Menci N., 2005, ApJ, 619, 60
McCarthy P. J. et al., 2004, ApJ, 614, L9
Maiolino R., Mannucci F., Baffa C., Gennari S., Oliva E., 2001, A&A, 372, L5
Maiolino R., Oliva E., Ghinassi F., Pedani M., Mannucci F., Mujica R., Juarez Y., 2004, A&A, 420, 889
Maiolino R. et al., 2005, A&A, 440, L51
Martin C. L., 2005, ApJ, 621, 227
Menci N., Fontana A., Giallongo E., Grazian A., Salimbeni S., 2006, ApJ, 647, 753
Narayanan D. et al., 2008, ApJS, 176, 331
Nesvadba N. P. H. et al., 2010, A&A, 521, A65
Nesvadba N. P. H., Polletta M., Lehnert M. D., Bergeron J., De Breuck C., Lagache G., Omont A., 2011, MNRAS, 415, 2359
Page M. J. et al., 2012, Nat, 485, 213
Rupke D. S. N., Veilleux S., 2011, ApJ, 729, L27
Saracco P. et al., 2005, MNRAS, 357, L40
Savage B. D., Sembach K. R., 1996, ARA&A, 34, 279
Silk J., Rees M. J., 1998, A&A, 331, L1
Springel V., Di Matteo T., Hernquist L., 2005, MNRAS, 361, 776
Steinhardt C. L., Silverman J. D., 2011, preprint (arXiv:1109.0537)
Sturm E. et al., 2011, ApJ, 733, L16
Thacker R. J., Scannapieco E., Couchman H. M. P., 2006, ApJ, 653, 86
Valiante R., Schneider R., Maiolino R., 2012, MNRAS, in press (arXiv:1205.3488)
Veilleux S., Cecil G., Bland-Hawthorn J., 2005, ARA&A, 43, 769
Walter F. et al., 2003, Nat, 424, 406
Walter F., Dahlem M., Lisenfeld U., 2004, ApJ, 606, 258
Walter F., Riechers D., Cox P., Neri R., Carilli C., Bertoldi F., Weiss A., Maiolino R., 2009, Nat, 457, 699
Weiß A., Neininger N., Hüttemeister S., Klein U., 2001, A&A, 365, 571
Wilson C. D. et al., 2008, ApJS, 178, 189
Zubovas K., King A., 2012, ApJ, 745, L34

This paper has been typeset from a TEX/LATEX file prepared by the author.